



HAL
open science

Size matters! Aurora A controls *Drosophila* larval development

Lucie Vaufrey, Christine Balducci, René Lafont, Claude Prigent, Stéphanie Le Bras

► **To cite this version:**

Lucie Vaufrey, Christine Balducci, René Lafont, Claude Prigent, Stéphanie Le Bras. Size matters! Aurora A controls *Drosophila* larval development. *Developmental Biology*, 2018, 440 (2), pp.88-98. 10.1016/j.ydbio.2018.05.005 . hal-01812516

HAL Id: hal-01812516

<https://univ-rennes.hal.science/hal-01812516>

Submitted on 4 Jul 2018

HAL is a multi-disciplinary open access archive for the deposit and dissemination of scientific research documents, whether they are published or not. The documents may come from teaching and research institutions in France or abroad, or from public or private research centers.

L'archive ouverte pluridisciplinaire **HAL**, est destinée au dépôt et à la diffusion de documents scientifiques de niveau recherche, publiés ou non, émanant des établissements d'enseignement et de recherche français ou étrangers, des laboratoires publics ou privés.

Size matters! Aurora A controls *Drosophila* larval development

Lucie Vaufrey^{1,2}, Christine Balducci³, René Lafont³, Claude Prigent^{1,2*}, Stéphanie Le Bras^{1,2*}

¹CNRS, UMR 6290, Équipe labellisée Ligue contre le Cancer 2014-2016, 35000 Rennes, France.

²Univ Rennes, IGDR (Institut de Génétique et Développement de Rennes), F-35000 Rennes, France.

³Sorbonne Université, IBPS (BIOSIPE), CNRS FR3631, 75005 Paris, France

lucie.vaufrey@laposte.net,

c.balducci@free.fr,

rene.lafont@upmc.fr

claud.prigent@univ-rennes1.fr

stephanie.lebras@univ-rennes1.fr

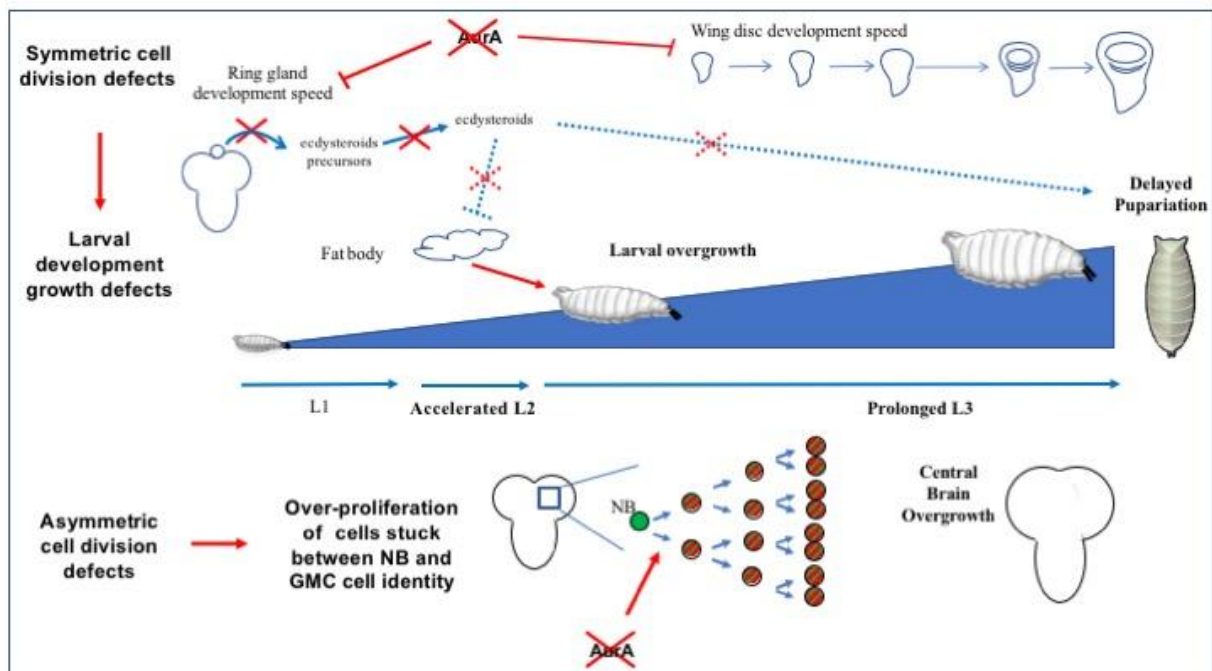
*Corresponding authors:

Abstract

In metazoans, organisms arising from a fertilized egg, the embryo will develop through multiple series of cell divisions, both symmetric and asymmetric, leading to differentiation. Aurora A is a serine threonine kinase highly involved in such divisions. While intensively studied at the cell biology level, its function in the development of a whole organism has been neglected. Here we investigated the pleiotropic effect of Aurora A loss-of-function in *Drosophila* larval early development. We report that Aurora A is required for proper larval development timing control through direct and indirect means. In larval tissues, Aurora A is required for proper symmetric division rate and eventually development speed as we observed in central brain, wing disc and ring gland. Moreover, Aurora A inactivation induces a reduction of ecdysteroids levels and a pupariation delay as an indirect consequence of ring gland development deceleration. Finally, although central brain development is initially restricted, we confirmed that brain lobe size eventually increases due to additive phenotypes: delayed pupariation and over-proliferation of cells with an intermediate cell-identity between neuroblast and ganglion mother cell resulting from defective asymmetric neuroblast cell division.

Keywords

Drosophila, Aurora A kinase, larval development coordination

Graphical abstract**1. Introduction**

Aurora kinases are essential guardians of cell cycle progression with multiple functions in mitosis/meiosis and interphase. They belong to a three member kinase family in mammals that evolved from a single yeast gene (*IPL1* in budding yeast and *ark1* in fission yeast) (Chan and Botstein, 1993; Petersen et al., 2001) that duplicated to give Aurora-A (AurA) and Aurora-B in worms, flies and amphibians. Later on, duplication of Aurora-B gave rise to Aurora-B and Aurora-C in mammals (Brown et al., 2004). Extensive studies in cellular models have revealed the pleiotropic and essential function of AurA during cell cycle. First, AurA plays a key role in the G2 to M transition by locally activating the phosphatase CDC25B and the kinase Plk1 (Dutertre et al., 2004; Macurek et al., 2008; Seki et al., 2008). Furthermore, during entry in mitosis, AurA is essential to centrosome maturation a

prerequisite to bipolar spindle assembly. Then during mitosis, the main role of the kinase is to control microtubule nucleation to successively assemble the bipolar spindle (Pinyol et al., 2013; Sardon et al., 2008) and the central spindle (Lioutas and Vernos, 2013; Reboutier et al., 2013). Finally, in G1 during interphase, the kinase participates in cilia resorption by activating the tubulin deacetylase HDAC6 (Pugacheva et al., 2007). Importantly, AurA is an oncogene frequently overexpressed in a large variety of cancers that has rapidly become a priority target for the development of inhibitors for the use in cancer treatment (Damodaran et al., 2017). Therefore, studies of its functions in any organism will impact cancer research due to the conserved nature of this kinase throughout evolution (Carmena et al., 2015).

Studies in organism models have demonstrated that AurA has essential functions during the cell cycle that are required for proper development as described in both vertebrates and invertebrates. In mice, knock-out of AURKA leads to preimplantation lethality with cell cycle defects in mitosis entry timing, bi-polar spindle assembly or chromosome segregation (Cowley et al., 2009; Lu et al., 2008; Sasai et al., 2008). The fact that knock-out embryos are able to reach the blastocyst stage can be attributed to residual maternal mRNA and/or protein AurA (Yao et al., 2004). Conditional knock-out of AURKA in different embryonic layers and/or at different post-implantation stages induces mitotic delay, increased apoptosis and early embryonic lethality which further supports the essential nature of AurA function during the cell cycle in development (Cowley et al., 2009; Yoon et al., 2012). Similarly, *zfAurora-A* depletion in zebrafish embryos also leads to embryonic lethality with similar mitotic failures (Jeon and Lee, 2013). Outstandingly, mutants are able to achieve embryonic but also larval development in *Caenorhabditis elegans* (*air1*) and *Drosophila melanogaster* (*aurA*) (Furuta et al., 2002; Glover et al., 1995) presumably thanks to the maternal contribution, as embryonic RNAi in *C. elegans* or maternal depletion in *drosophila* leads to defective mitosis and eventually embryonic lethality (Glover et al., 1995; Schumacher et al., 1998). In *C. elegans*, mutants reach the adult stage with mitotic defects as reported in the ventral cord and vulva lineages (Furuta et al., 2002). On the contrary, *Drosophila* mutants do not reach the adult stage and die at the pupal stage during metamorphosis (Glover et al., 1995; Lee et al., 2006; Moon and Matsuzaki, 2013; Wang et al., 2006). The fact that *Drosophila aurA* loss-of-function (*aurA^{lof}*) mutants survive throughout larval development can be explained by larval growth reliance on increasing polyploidy in larval tissues (Royzman et al., 1997) and not on mitotic tissues (central nervous system and imaginal discs) of which correct development is eventually essential during pupal metamorphosis (Shearn and Garen, 1974). In accordance with this hypothesis, most essential cell cycle regulators have been identified in genetic

screens based on late larval/pupal lethality linked to defects in cell division of larval imaginal tissues (Gatti and Baker, 1989). Surprisingly, the only defects reported in *Drosophila aurA^{lof}* mutant larvae are in central nervous system neuroblasts (NB) while no defect were observed in other larval tissues included imaginal discs which divide intensively during larval development (Lee et al., 2006; Moon and Matsuzaki, 2013; Wang et al., 2006). Still, *aurA^{lof}* mutant NB share features of mitotic defects such as delayed mitosis entry, defective centrosomes number and chromosome mis-segregation, a trademark of AurA loss-of-function (Caous et al., 2015; Lee et al., 2006; Wang et al., 2006).

NB are progenitors of the central nervous system lineages which divide asymmetrically to renew a NB and to produce a ganglion mother cell (GMC) that will divide and produce the multitude of neurons and glial cells (for review see (Kang and Reichert, 2015)). During embryonic development, NB delaminate from the neuroectoderm and divide asymmetrically until they enter quiescence by the end of embryogenesis (Lai and Doe, 2014; Tsuji et al., 2008). During larval development, embryonic NB exit quiescence and divide asymmetrically in the central brain and ventral nerve cord while new NB delaminate and first start dividing symmetrically then asymmetrically in the optic lobe. The central brain NB exit from quiescence takes place from the late 1st instar larval (L1) stage (Britton and Edgar, 1998; Green et al., 1993; Hartenstein and Campos-Ortega, 1984) and is timely controlled in part by glial cells (Datta, 1995; Ebens et al., 1993; Voigt et al., 2002) which relay a nutrition-dependent fat body derived signal (Sousa-Nunes et al., 2011). Fat-body derived signals controlling systemic growth have recently been identified but it remains to be demonstrated that they actually control NB quiescence exit (Koyoma and Mirth, 2016; Delanoue et al., 2016). Central brain NB further divide asymmetrically and reach a plateau of extensive division during the 3rd instar larval (L3) stage until pupariation (Ito and Hotta, 1992). In *aurA^{lof}* mutants (*aurA⁸⁸³⁹*, *aurA¹⁴⁶⁴¹* and *aurAST*), brain lobes of wandering L3 larvae reach up to 10 times the volume of control larvae, have too many larval pseudo-NB (cells positive for NB markers and which can divide symmetrically) resulting from defective NB asymmetric cell division and are highly tumorigenic (Caous et al., 2015; Lee et al., 2006; Moon and Matsuzaki, 2013; Wang et al., 2006). Based on these observations, *aurA* is defined as a brain tumor-suppressor gene in *Drosophila*. However, other *Drosophila* brain tumor-suppressor genes are also imaginal disc tumor-suppressor genes (Gateff, 1994), which has not been reported in *aurA^{lof}* mutants. Therefore, we decided to examine the AurA tumor-suppressor property in other tissues and search for additive phenotypes in *aurA^{lof}* mutants that could contribute to NB-like over-proliferation. We investigated *aurA^{lof}* phenotypes from the

beginning of larval development as all previous studies were performed at the end of the L3 stage (wandering L3 stage). Here, we revealed that AurA is actually a regulator of different larval development processes including the regulation of larval growth rate and pupariation timing. Furthermore, we could identify that *aurA* does not act as a tumor-suppressor cell-autonomously in larval NB as previously described. Instead, in the absence of AurA function, NB give rise to cells with an intermediate cell-identity between NB and GMC which escape a spatio-temporal control of the number of cell divisions rounds.

2. Material and Methods

2.1. *Drosophila* strains and genetics.

Origin of all stocks and details of all crosses are listed in Supplementary table 1 and 2.

*w*¹¹¹⁸ was used as wild-type control for all experiments.

Five *aurA* alleles, which are all late larval/early pupal lethal (data not shown), were used in this study: *aurA*¹⁴⁶⁴¹ a hypomorph EMS mutant (Lee et al., 2006; Wang et al., 2006); *aurA*⁸⁸³⁹ a strong hypomorph EMS mutant (Lee et al., 2006; Wang et al., 2006); *aurA*^{3A} and *aurA*^{3C} are CRISPR indels (Aurore Dussert and Roland Le Borgne, personal communication). *aurA*^{3A} has a 7-bp deletion resulting in a frame-shift F177SWWterm and *aurA*^{3C} has a 15-bp deletion resulting in a 5-aa deletion (Δ 175-180:ESQFV); *aurA*ST a null mutant resulting from a P-element excision, which can be rescued by expressing *aurA* with *arm*-GAL4 (Moon and Matsuzaki, 2013). To bypass any EMS- or CRISPR- related off-target effects, all experiments were performed in trans-heterozygous genotypes with the *aurA*ST allele.

For clonal analyses, *hs*-FLP; FRT[82B] *ubi*-nls::RFP were crossed with *w*; FRT[82B], *aurA*ST or *w*; FRT[82B]. Embryos were laid for 4h and heat-shocked at 37°C during 1h at 48h after egg laying (AEL). Tissue dissection and immunostaining were performed in wandering L3 larvae at 120h AEL. Only clones of type I neuroblasts recognizable by the presence of large deadpan-positive neuroblasts and/or their ventral localization in the central brain were observed in this study.

The avalanche RNAi experiment was performed at 25°C as previously described (Colombani et al., 2012) and with the following genotype: *w*; *elav*-GAL80; *Rn*-GAL4, UAS-*Avl*^{dsRNA} / TM6b, *tub*-GAL80. RNAi experiments to study pupariation delay were performed at 25°C with the following drivers: ubiquitous (69B-GAL4 and *arm*-GAL4), ring gland-specific (*phm*-GAL4), peripheral tissue-specific (*ppl*-GAL4), fat-body specific (*lpp*-GAL4), neuroblasts-specific (*wor*-GAL4) and wing-disc specific (*pdm2*-GAL4 and *ser*-GAL4); and UAS-dsRNA lines: UAS-*aurA*^{dsRNA} and UAS-*white*^{dsRNA} (see supplementary table 1 for genotype details).

2.2. RT-PCR

RNA was extracted from 30 central brains of wandering L3 larvae after dissection in PBS and with a RNA isolation kit from Zymo Research. 3 µg of total RNA was used for reverse transcriptase reaction performed in a final volume of 20 µl during 1h at 50°C using oligodT primer and Superscript III Reverse Transcription (Thermo Fisher Scientific). 2 µl of each RT reaction were used for PCR using the following primers:

<i>tubulin</i> , forward	5'-TCCTTGTCGCGTGTGAAACA-3'
<i>tubulin</i> , reverse	5'-AGCTTGGACTTCTTGCCGTA-3'
<i>aurA</i> exon 1 to 2, forward	5'-CTGTTAGTTGTCGAGTGCCT-3'
<i>aurA</i> exon 1 to 2, reverse	5'-CAGCAGGCGACCAATATCAA-3'
<i>aurA</i> exon 3, forward	5'-TTGATATTGGTCGCCTGCTG-3'
<i>aurA</i> exon 3, reverse	5'-AATGTGTTCACTGCGTGTGC-3'
<i>aurA</i> exon 1 to 3, forward	5'-CTGTTAGTTGTCGAGTGCCT-3'
<i>aurA</i> exon 1 to 3, reverse	5'-AATGTGTTCACTGCGTGTGC-3'

2.3. *AurA* antibody, protein production, kinase assay and western blot

Polyclonal anti-*AurA* antibodies were produced in rabbit against the amino acids 1-15: MSHPSDHVLRPKENA and ordered from Eurogentec.

Proteins were extracted from wandering L3 larvae as following: 20 brains were dissected in PBS and incubated with vortex for 30min in cold buffer lysis (50 mM Tris-HCl pH 7,4; 150 mM NaCl; 1% TritonX-100; 1.5 mM MgCl₂; 0.2 mM Na₃VO₄; 0.5 mM DTT, 4 mg/mL NaF; 5.4 mg/mL β-GlycerolPhosphate, cOmplete™ Protease Inhibitor Cocktail (Roche). After 30min of centrifugation at 13000 rpm, 4°C, supernatant was quantified with the Pierce™ BCA Protein Assay Kit (ThermoFisher). 50 µg of proteins diluted in Laemmli buffer was loaded onto Mini-PROTEAN® TGX™ 4-15% gels (BioRad), transferred onto a PVDF membrane (GE Healthcare) and detected using the following antibodies: rabbit anti-*AurA* (1:10000, this paper), rabbit anti-actin (1:1000, Sigma Aldrich) and HRP-conjugated secondary antibodies, 1:5000 (Molecular Probes).

To express recombinant 6xHis-*AurA* proteins, coding sequences of wild type or mutant *aurA* were cloned into pET15g plasmid (a gift from Gwenaël Rabut) using the cDNA #LD16949 (cDNA ReSource Center) as a matrix and the following primers: 5'-GAAAACCTGTATTTTCAGATGTCCCATCCGTCT-3' (forward) and 5'-GACCTAGGCTCGAGATCACTGCGTGTGCGC-3' (*aurA*^{WT} reverse) or 5'-

GACCTAGGCTCGAGACTAGGAAATGTGCTCCGG-3' (*aurA*⁸⁸³⁹ reverse). Gibson Assembly Master Mix (NEB) was used to clone mutant *aurA* using the following primers for intermediate amplicons: for *aurA*^{3A} 5'-CGCGGGAAAAGGAATGTGGTGGCCCTAAAA-3' (forward) and 5'-TTTTAGGGCCACCACATTCCTTTTCCCGCG-3' (reverse); for *aurA*¹⁴⁶⁴¹ 5'-GGTTGGTCCGAGCACGAGCCG-3' (forward) and 5'-CGGCTCGTGCTCGGACCAAC-3' (reverse) and for *aurA*^{3C} 5'-CGTTTCGGGAAAAGGTGGCCCTAAAAGTG-3' (forward) and 5'-CACTTTTAGGGCCACCTTTTCCCGAAACG-3' (reverse).

Protein purification and kinase assay with histone H3 were done as previously described (Bertolin et al., 2016). Briefly, BL21(DE3) *E.coli* strains (New England Biolabs, NEB) are transformed with pET15g-Aurora A plasmid and induced with 0.5 mM isopropyl β -D-1-thiogalactopyranoside for 16h at 20°C. After lysis and sonication, supernatants were incubated with Nickel-chelating resin (ProBond, Thermo Fisher Scientific) for 1h at 4°C under gentle rotation and proteins were purified under native conditions. For the kinase assay reaction, 10 pmol of purified Histone H3 and/or 10 pmol of purified wild-type or mutant Aurora-A protein were added to kinase buffer (50 mM Tris-HCl (pH 7.5), 25 mM NaCl, 10 mM MgCl₂, 1 mM dithiothreitol and 0.01% Triton X-100) with or without 100 μ M ATP. The reaction was incubated for 20min at 37°C and 10 μ L was analyzed by western-blot using rabbit anti-Histone H3 pSer10 (1:1000, Merck Millipore, 06-570). Red Ponceau was used to control the amount of total proteins.

2.4. Crosses for larvae measurement, larvae staging and pupariation temporal analyses.

All crosses were performed in parallel with controls on the same standard food Nutri-FlyTM Bloomington Formulation (Flystuff, Genesee Scientific) under constant light at 25°C. For each genotype, 15 virgins of *aurA*ST / TM6 *Tb*⁻ *Sb*⁻ or GAL4 lines were crossed with 5 males of *aurA*^{lof} / TM6 *Tb*⁻ *Sb*⁻ or UAS-*dsRNA* lines. For all following experiments, embryos were laid for 4h in standard food tube. *Tb*⁻ was used to distinguish sibling larvae from mutant ones while *Sb*⁻ marker was used for sibling adult flies.

For larval size measurement and staging, larvae were collected from food at given time points and left in cold PBS until no movement was observed. Larvae pictures were taken with a Leica DFC420 macroscope and staged in respect with anterior and posterior spiracles larval development independently from their size: L1 have white posterior spiracles, L2 have orange posterior spiracles and apparition of club shaped anterior spiracles, early L3 have branched

anterior spiracles, late L3 have everted anterior spiracles and wandering L3 are found out of the food (Park et al., 2002).

For pupariation delay quantification, white pupae were counted every 24 h until no wandering L3 larvae were visible for at least 48h in the laying tube. Pupae were individually collected in a plastic plate with humid paper to allow complete metamorphosis. 100% of pupariation was defined as the total of white pupae counted for one given cross per experiment.

2.5. *Ecdysteroids quantification by LC-MS/MS*

For time course experiments between 72 and 192 h after egg laying (AEL), groups of larvae were collected every 12 hours from 6 to 8 independent crosses and pooled in groups of at least 30 larvae. At given time points, “not wandering” and “wandering” L3 larvae were collected in different tubes and considered as different stage points. For each time and/or stage points, ecdysteroids were quantified from two to four independent pools of larvae with the following protocol adapted from (Lavrynenko et al., 2015).

Larvae were transferred into CK14 tubes (Ozyme) containing ceramic beads and 500 μ L methanol (MeOH) was added. Tubes were inserted in a FastPrep FP120 (Savant Bio101) and agitated for 30 seconds. After centrifugation, pellets were re-extracted with 400 μ L MeOH and vortexed. After centrifugation, pellets were once again re-suspended in 400 μ L MeOH, vortexed and sonicated for 5min. The three supernatants were mixed, 25 ng of polypodine B (internal standard) was added and the extracts were evaporated until dry using a EZ2 (Genevac) vacuum evaporator without heating for 2 h. Residues were then re-dissolved with 80 μ L MeOH/H₂O (1:1) and centrifuged. HPLC-MS/MS analyses was performed with a QQQ Mass Spectrometer 6420 (Agilent Technologies) in the ESI mode. The HPLC apparatus comprised a quaternary pump G13118 and a multisampler injector G7167 (Agilent). Separation was performed in a column Fortis C18 50 mm long, 2.1 mm i.d. (5 μ m particles), temperature 30°C, flow-rate 0.3 mL/min, gradient 10% to 90% (in 5min) of acetonitrile in water containing 0.1% formic acid. Injection volumes: 15 μ L. Detection used MRM transitions in the positive (M+H)⁺ mode. The transitions used were respectively 481.1 \rightarrow 371.2 (20E), 495.1 \rightarrow 459.3 (makisterone A) and 497.4 \rightarrow 351.3 (polypodine B). Calibration curves were made from stock solutions (5 mg/mL DMSO) of makisterone A and 20E diluted with MeOH, and gave a linear curve in the range 5-5000 ng/mL. The limit of quantification (LOQ) was 5 ng/mL. Reference ecdysteroids: 20E, makisterone A and polypodine B (purity > 98%) were obtained from various plant sources and purified by BIOSIPE lab.

2.6. *Larval tissues immunostaining*

The following antibodies (dilution, source) were used: rat anti-Deadpan (1:50, 11D1BC7, Abcam), rat anti-Elav (1:50, 7E8A10, Developmental Studies Hybridoma Bank/DSHB), rabbit anti-pH3 (1:1000, Upstate) and mouse anti-Prospero (1:1000, MR1A, DSHB). Fluorescently conjugated 488-, 546- and 647- secondary antibodies (Invitrogen) were used at 1:250. Larval tissues from timed and/or staged larvae were dissected in phosphate-buffered saline (PBS) and fixed for 15min in 4% formaldehyde. Tissues were washed in PBS with 0.1% Triton X-100 (PBT) for 10min and incubated overnight with primary antibodies at 4°C under agitation. Tissues were washed in PBT and incubated with secondary antibodies at room temperature. When Hoescht was used, tissues were rinsed once in PBT and incubated 10min with Hoescht (1:100000). Tissues were washed in PBS for 10min and mounted in glycerol 90% with 2.5% DABCO. All brains were mounted with dorsal surface up and ventral surface down.

2.7. Confocal Microscopy

Fluorescent images were acquired with a Leica SP8 confocal equipped with a 20X, 40X or 63X objectives and a laser module (excitation at 405, 488, 561 and 633 nm) at the Microscopy Rennes imaging Center. Z stacks were recorded at 0.5 μm intervals. Confocal and DIC images were acquired and processed using the LAS AF software and further analyzed with ImageJ. Wing disc, ring gland and central brain circumferences were measured using Polygon selection and Measure tools from ImageJ.

2.8. Statistical analyses

Statistics were performed on RStudio using Mann-Whitney test to compare two specific datasets. Multiple comparison within a given dataset (with different *aurA*^{lof} genotypes or time points) was performed with a Mann-Whitney non-parametric test as the variances of data sets were not equal (tested with a Barlett test), $p < 0.05$ when data of two sets are significantly different, $p < 0.025$ for data of three sets and $p < 0.0125$ for data of five sets. Comparison of nuclei density in ring glands of given genotypes was performed with a Two-sample Kolmogorov-Smirnov test, $p < 0.05$ when data of two sets are significantly different.

3. Results

3.1. *Drosophila* larval development is temporally affected in the absence of AurA kinase activity.

In order to investigate *aurA*^{lof} phenotypes during larval development we took advantage of an allelic series: *aurA*^{3A}, *aurA*⁸⁸³⁹, *aurA*^{3C} and *aurA*¹⁴⁶⁴¹ and one null mutant, *aurA*ST (Fig. 1A). AurA mRNA is detected for all mutants excepted *aurA*ST (Sup. Fig. 1A), while AurA protein

is detectable at the expected size for $aurA^{8839}$, $aurA^{3C}$ and $aurA^{14641}$ and absent for $aurA^{ST}$ and $aurA^{3A}$ (Fig. 1B). The fact that the antibody we used is able to detect the $AurA^{3A}$ protein isoform expressed in bacteria, confirms that no $AurA$ protein were detectable in $aurA^{3A}$ mutants (Sup. Fig.1B). We further characterized these $AurA$ mutant proteins by measuring their kinase activity *in vitro* towards histone H3 Serine10, a classical *in vitro* substrate of $AurA$ (Hsu et al., 2000). We could not detect any kinase activity for any of these $AurA$ mutant forms while we did for the wild-type isoform (Sup. Fig. 1C). Therefore, the allelic series includes mutants with or without $AurA$ proteins but all depleted of detectable $AurA$ kinase activity.

We then analyzed *Drosophila* early development and strikingly found that all mutants show a delay in pupariation despite the variability observed at different time points for a given genotype (Fig. 1C). Although the expressivity of this phenotype is variable between mutants, they all present a clear delay in pupariation as visible at 144h after egg laying (144h AEL) when the mean of control genotypes has surpassed 50% of pupariation. We decided to pursue the study with the null allele $aurA^{3A}$, which present the strongest delay and has no detectable protein, and the hypomorph $aurA^{14641}$, which has the weakest delay and expresses a kinase dead protein. In physiological conditions, larval development starts at 24h AEL and is temporally stereotyped. It lasts for four days and is divided into four stages of 24h each; 1st instar (L1), 2nd instar (L2), early 3rd instar (early L3) and late 3rd instar (late L3) including the wandering L3 stage where larvae start crawling prior to pupariation (Fig. 1D). To identify how larval development of $aurA^{lof}$ mutants is temporally affected, we evaluated the larval stages reached every 24h (Fig. 1E). Surprisingly, we first noticed that mutant larvae are predominantly already in L3 stages at 72h AEL (62% for $aurA^{3A/ST}$, $n_{total}=48$ and 72% for $aurA^{14641/ST}$, $n_{total}=40$) when controls are for the most part in L2 stage (75%, $n_{total}=138$). Nonetheless, mutant larvae are still in L3 stages at 120h AEL (100% for $aurA^{3A/ST}$, $n_{total}=59$ and 100% for $aurA^{14641/ST}$, $n_{total}=56$) when 36% of controls ($n_{total}=183$) have already reached the pupal stage. Furthermore, the control shows 62% pupae ($n_{total}=214$) at 144h AEL while the hypomorph $aurA^{14641/ST}$ expressing the inactive kinase shows 31% pupae ($n_{total}=29$) and the null $aurA^{3A/ST}$ remain in L3 (100%, $n_{total}=27$). At 168h AEL controls show 100% pupae ($n_{total}=121$), the hypomorph $aurA^{14641/ST}$ 88% pupae ($n_{total}=34$) while the null $aurA^{3A/ST}$ only 29% ($n_{total}=24$). These data show that loss of $aurA$ function increases the duration of L3 stage and that the effect is more pronounced with the null mutant ($aurA^{3A/ST}$) compared to the mutant expressing the inactive kinase ($aurA^{14641/ST}$).

3.2. *aurA* loss-of-function affects ring gland development which in turns alters ecdysteroids production and larval growth rate and speed.

Extension of the L3 stage usually correlates with a phenotype of enlarged larvae due to a longer duration of larval feeding (McBrayer et al., 2007). As predicted, *aurA*^{lof} mutant L3 larvae are bigger than control L3 larvae at 120h AEL (Fig. 2A and sup. Fig.2A). However, larger larvae are already observed in *aurA*^{lof} mutants at 72h AEL (Fig. 2A and sup. Fig. 2A). Noteworthy, the majority of control larvae are in L2 stage at 72h AEL while the majority of *aurA*^{lof} mutants have already reached the L3 stage (Fig. 1E), which could explain the larval size difference. To circumvent this bias of accelerated early larval development in *aurA*^{lof}, we compared the size of larvae at given larval stages rather than at given developmental time points (Fig. 2B and sup. Fig. 2B). At both L2 and late L3 stages, *aurA*^{lof} mutant larvae sizes are bigger than the controls (Fig. 2C) which confirm that *aurA*^{lof} mutant systemic growth is accelerated from the L2 stage.

Early larval growth rate and speed are dependent upon ring gland development and ecdysteroids production. Indeed, defective growth and/or reduction of insulin/Pi3K growth-promoting signaling pathway in ring gland inhibit early release of ecdysteroids required in the fat body to restrict early larval systemic growth (Colombani et al., 2005; Mirth et al., 2005). Furthermore, the precise timing of each molt (L1/L2 and L2/L3), and the onset of metamorphosis, are finely regulated in a stereotyped manner by pulses of ecdysteroid hormones (Riddiford, 1993). If the ecdysteroids synthesis pathway is affected, it induces a gradient of phenotypes ranging from delayed-L1 to pupal-lethal through arrested-L3 (Danielsen et al., 2016). We reasoned that both ecdysteroid-related phenotypes *aka* increased larval body size (Fig. 2B) and pupariation delay (Fig. 1C) could reflect a defect in ecdysteroids production. Using quantitative liquid chromatography-tandem mass spectrometry (LC-MS/MS), we quantified the temporal profiles of 20E and Maki-A in control and *aurA*^{lof} mutant larvae from 72h AEL (stage L2) until larvae reach the wandering L3 stage (Sup. Fig. 3A and B). In *aurA*^{3A/ST} mutants, we observed a clear deficit in 20E and Maki-A amounts despite the strong variability at each time points. In control larvae, “not wandering” and “wandering” L3 larvae were present at each time points from 96h AEL which might explain the observed variability of ecdysteroids quantity. Therefore, we discriminated the results of “not wandering” L3 vs “wandering” L3 for control and *aurA*^{3A/ST} mutant larvae by pooling our quantification results from 96h AEL (Fig. 2C). Basal levels of ecdysteroids were observed in “not wandering” L3 *aurA*^{3A/ST} mutants but the major peak was not observed in “wandering” L3, which confirms that AurA is required for ecdysteroids production.

While ecdysteroid precursors, Ecdysone and 24-methylecdysone, are produced in the prothoracic gland (PG) of the ring gland, they are rapidly converted into the main active molting hormones, 20-Hydroxyecdysone (20E) and Makisterone A (Maki-A) respectively, in peripheral tissues including the fat body (reviewed in Lafont et al., 2017). To identify the organ(s) in which AurA activity is required for this ecdysteroids major peak production, we inactivated *aurA* in the ring gland or the peripheral tissues. We used the UAS/GAL4 system to induce RNA inactivation (RNAi) specifically in these tissues and search for one of the readouts of defective ecdysteroids production: a pupariation delay. Although we observed a limited effect when inactivating *aurA* in peripheral tissues (Ballard et al., 2010) using a *pumpless* (*ppl*)-GAL4 driver (Sup. Fig. 4B), pupariation was delayed when *aurA* was inactivated in the PG using a *phantom* (*phm*)-GAL4 driver (Fig. 2D). As AurA function appears essential in the ring gland, we looked ring gland larval development in *aurA*^{lof} mutants. We could not easily dissect the ring gland at early stage due to its smaller size in mutants (not shown) but at 120h AEL, ring gland was measurably smaller in *aurA*^{lof} mutants compared to controls (Fig. 2E-F and Sup. Fig. 3C). However, it was already reported that it is not the size of the ring gland that matters for ecdysteroids production (Colombani et al., 2005) but rather the endocycle progression of cells in the PG (Ohhara et al., 2017). At 120h AEL, cells of the *aurA*^{3A/ST} mutant PG are still mitotic while very few mitotic figures are observed in control PG (Sup. Fig 3D). To evaluate the endocycle progression of PG cells, we measured the size of their nucleus (Fig 2H). At 120h AEL, nuclei size density does not follow a Gaussian distribution in late L3 *aurA*^{3A/ST} mutants compared to wandering L3 controls. However, at 144h AEL (late L3) and 168h AEL (wandering L3), the nuclei size density distribution of mutants tends to resemble the controls while almost no mitotic figures were observed (Fig 2G). In conclusion, loss of *aurA* function reduces ring gland developmental speed presumably by slowing down cell cycle speed and thus delaying endocycle progression. Consequently, AurA kinase activity is required for the major peak of ecdysteroids production controlling the timing of pupariation.

3.3. *aurA* loss-of-function affects wing disc development rate and speed

Although it has been previously described that imaginal disc development is not altered in wandering L3 larvae of *aurA* mutants (*aurA*⁸⁸³⁹, *aurA*¹⁴⁶⁴¹ and *aurA*ST, (Lee et al., 2006; Moon and Matsuzaki, 2013)), we wondered if it could be defective at earlier larval stages and if these defects could have been rescued during the prolonged L3 stage and then missed in wandering L3 *aurA*^{lof} mutants. As wing disc development reaches its maximum speed during

L3 stage, we looked at them from the beginning of L3 stage in *aurA^{lof}* mutants. We were unable to dissect *aurA^{lof}* mutant wing discs at 96h AEL as we could not identify them with enough confidence due to their small size and their unidentifiable morphology (data not shown). At 120h AEL (Fig. 3A), we observed that wing discs of “not wandering” L3 *aurA^{lof}* mutant larvae are smaller than “wandering” L3 controls ($p=4.72 \times 10^{-6}$ for *aurA^{3A/ST}*, $n=37$ and $p=5.26 \times 10^{-3}$ for *aurA^{14641/ST}*, $n=35$), while the difference is mostly abolished at 168h AEL between “wandering” L3 *aurA^{lof}* mutant and controls ($p=2.43 \times 10^{-3}$ for *aurA^{3A/ST}*, $n=20$ and $p=0.94$ for *aurA^{14641/ST}*, $n=16$). Furthermore, wing disc morphology is also initially altered in *aurA^{3A/ST}* mutants as the wing pouch is rarely detected in wing discs before 168h AEL ($n=4/37$ at 120h AEL and $n=17/20$ at 168h AEL in mutants, Fig. 3D,G) while it is visible in *aurA^{14641/ST}* mutant wing discs (Fig. 3C,F) and control wing discs from 120h AEL (Fig. 3B,E). These observations demonstrate that loss of *aurA* reduces wing disc development and that wing discs take advantage of the prolonged L3 stage to recover and resume normal development (size and morphology). Again, as observed for the pupariation delay, the phenotype observed in the mutant *aurA^{14641/ST}* (inactive kinase) is less pronounced than that of the mutant *aurA^{3A/ST}* (no protein), which further supports the link between *aurA* loss-of-function and reduction of wing disc growth speed.

The deceleration of wing disc development can result from the reduction of ecdysteroid levels (Herboso et al., 2015) and/or cell-autonomous defects. Indeed, loss of AurA kinase activity increases cell cycle length by decelerating the entry into and progression through mitosis (Caous et al., 2015; Lim et al., 2017), which could explain the fact that wing discs need more time to achieve their development in *aurA^{lof}* mutant larvae. To bypass the ecdysteroids defect effect, we performed a clonal analysis to compare the multiplication rate of *aurAST* homozygous mutant cells and wild-type sibling cells, which derive from heterozygous mother cells after induced recombination (Xu and Rubin, 1993). We observed that *aurAST* homozygous mutant clones were significantly smaller than their wild-type siblings (Fig. 2I' versus 2J' and 2K), which demonstrates that *aurAST* wing disc cells divide at a smaller rate than their wild-type siblings. Furthermore, the mitotic index was higher in *aurAST* clones than in wild-type clones (Fig. 2G-H), which confirms that *aurA* loss-of-function affects wing disc development in a cell-autonomous manner.

In case of an alteration of wing disc development, wing disc cells produce an excess of Dilp8 which activates leucine-rich repeat-containing G protein-coupled receptor 3 (LgR3)-neurons to delay pupariation until wing disc development is corrected (Colombani et al., 2015; Garelli et al., 2015). These LgR3 neurons inhibit two pairs of central brain neurons, which innervate

the PG and produce the prothoracicotropic hormone required for pupariation-inducing ecdysteroids release in wandering L3 larvae (McBrayer et al., 2007; Warren et al., 2006). To test if the Dilp8-LgR3 pathway could be activated in *aurA^{lof}* mutants, we specifically inactivated *aurA* in the wing discs by RNAi using two different GAL4 drivers: *serrate* (*ser*) and *pdm2*. Although we observed wing margin phenotypes (data not shown), inactivation of *aurA* was not sufficient to induce a pupariation delay and validate this hypothesis (Sup. Fig. 4E,F). Together, these data show that loss of *aurA* function reduces wing disc development speed by slowing down cell cycle speed and the pupariation delay allows for correction of this developmental defect.

3.4. *aurA* is required for NB-cell lineage differentiation in larval central brain.

Examining AurA function during early *Drosophila* development helped us to define its pleiotropic roles with multiple phenotypic readouts. Indeed, *aurA^{lof}* larval developmental rate and speed defects might result indirectly from primary growth defects in the ring gland (Fig. 2) while wing disc development deceleration results from cell-cycle cell-autonomous defects (Fig. 3). It has been previously reported that the volume of the brain lobes of wandering L3 larvae in *aurA^{lof}* mutants is much greater than that of the controls and is correlated with a huge number of NB (Lee et al., 2006; Moon and Matsuzaki, 2013; Wang et al., 2006). To test if the increased brain lobe size is directly due to the larger size of the *aurA^{lof}* mutant larvae (Fig. 2B), we measured brain lobe circumferences in another genetic background with enlarged larval size. We took advantage of a validated genetic model in which RNAi of *avalanche* (*avl*) in imaginal discs induces a delayed L3 stage and enlarged larvae (Colombani et al., 2012). Although *aurA^{lof}* mutants and *avl^{dsRNA}* larvae have the same enlarged larval size at 120h AEL (Sup. Fig. 5A), brain lobe sizes are smaller than controls in both genotypes (Sup. Fig. 5B). In later stages (144h and 168h AEL) when *aur^{lof}* and *avl^{dsRNA}* have reached the wandering stage, brain lobes are still smaller than controls in *avl^{dsRNA}* while they become much larger in *aur^{lof}* (Sup. Fig. 5B). Therefore, the enlarged brain lobes phenotype does not appear to be a direct consequence of increased larval growth and/or prolonged L3 stage. Surprised by the initial smaller size of *aur^{lof}* brain lobes, we questioned whether the growth rate of brain lobes could be decreased during early larval development as observed in the ring gland. In fact, brain lobe perimeters are significantly smaller in *aurA^{3A/ST}* and to a less extent in *aurA^{14641/ST}* mutants in early and late L3 stages at 96h AEL (Fig. 4A, $p=2.85 \times 10^{-7}$ for *aurA^{3A/ST}*, $n=33$ and $p=0.03$ for *aurA^{14641/ST}*, $n=33$). Then, brain lobe perimeters progressively increase during *aurA^{lof}* L3 stage and eventually become bigger than controls, as previously

described, in wandering L3 mutant larvae at 192h AEL (Fig. 4A, $p=2.85 \times 10^{-7}$ for $aurA^{3A/ST}$, $n=47$ and $p=0.03$ for $aurA^{14641/ST}$, $n=8$ and Sup. Fig. 6A-G). We confirmed these results with our allelic series: brain lobes sizes are indeed initially smaller in early larval development and become bigger in latest stages independently of the allelic combination which further highlights an early larval function for AurA in brain development (Sup. Fig. 6A). Numerous previous studies have shown that this enlarged brain phenotype of $aurA^{lof}$ wandering larvae is correlated with a huge number of NB in which the length of the cell cycle is increased due to a delay of entry into mitosis (Caous et al., 2015; Lee et al., 2006; Lim et al., 2017; Moon and Matsuzaki, 2013; Wang et al., 2006). As central brain NB exit quiescence around 48h AEL at the end of L1 (Ding et al., 2016; Sousa-Nunes et al., 2011), we looked at the number of cells positive for Deadpan (Dpn), a marker of NB-cell identity, in the central brain from 48h AEL (end of L1). To our surprise, the number of Dpn-positive (Dpn^+) cells appeared higher in $aurA^{3A/ST}$ brain lobes of L2/L3 stages at 72h AEL (Fig. 4C,F) and increased in such a dramatic way that Dpn^+ cells cannot be counted unambiguously in L3 stages at 120h AEL (Fig. 4D,G) when brain lobes are still smaller than the control (Sup. Fig. 6A). Furthermore, the central brain organization is highly affected in $aurA^{3A/ST}$ mutants and the optic lobe is not always distinguishable at 120h AEL ($n=12/30$ central brains, three experiments, data not shown). Together, these data correlate with a defect in NB-cell lineage differentiation. Indeed, as described for other $aurA^{lof}$ mutant alleles, the number of neurons (marked by Embryonic Lethal Abnormal Visual system, ELAV, a neuron-specific protein) is strongly reduced in $aurA^{3A/ST}$ brain lobes (Sup. Fig. 6H,I and (Lee et al., 2006; Wang et al., 2006)). Furthermore, we observed a large quantity of cells with a small nucleus positive for both Dpn and Prospero (Dpn^+ , $Pros^+$) in $aurA^{3A/ST}$ brain lobes (Sup. Fig. 6F,G). These cells originate from defective NB asymmetric cell divisions which give rise to two (small nucleus, Dpn^+ , $Pros^+$) identical cells (Lee et al., 2006; Wang et al., 2006; Wirtz-Peitz et al., 2008) (referred to as NB-GMC-like cells hereafter). To confirm that a complete loss of $aurA$ function impairs NB-cell lineage, we used clonal analysis. In wild-type clone, we can observe one NB which recently divided (large nucleus, Dpn^+ , $Pros^+$) is seen with one new GMC (small nucleus, Dpn^+ , $pros^+$) and numerous older GMC (small nucleus, Dpn^- , $Pros^+$) (Fig. 4H-H'''). In $aurA^{ST}$ mutant clone, one NB is seen with numerous NB-GMC-like cells (small nucleus, Dpn^+ , $Pros^+$) (Fig. 4I-I'''). Indeed, those NB-GMC-like cells is significantly increased in mutant clones (Fig. 4J, $p=1.2 \times 10^{-4}$, $n=14$). We also observed a small increase number of GMC (Dpn^- , $Pros^+$) cells in $aurA^{ST}$ mutant clones which suggest that mutant NB divided into NB-GMC-like cells which multiply and eventually give rise and/or differentiate into GMC (Fig. 4K, $p=0.069$, $n=14$). In

conclusion, AurA loss-of-kinase activity in central brain NB gives rise to cells with an intermediate identity between NB and GMC, which greatly proliferate during central brain larval development. In addition to the prolonged L3 stage, the proliferation of these NB-GMC-like eventually give rise to enlarged brain lobes in *aurA^{lof}* mutants.

Discussion

In this study of AurA function during the development of *Drosophila* larvae, we found that loss of AurA kinase activity results in pleiotropic effects in different tissues (ring gland, imaginal wing disc and central brain) and reduces their growth rate throughout larval development. In early larval development, AurA is first needed in the ring gland to control its growth speed. It is well established that a defect in early ring gland development affects the release of the ecdysteroid precursors by its PG cells and indirectly accelerates early larval growth rate and speed (Caldwell et al., 2005; Colombani et al., 2005; Mirth et al., 2005). Indeed, the hormones fulfill multiple functions such as the repression of larval growth by inhibiting dMyc expression, through its receptor EcR, in the fat body (Delanoue et al., 2010). Therefore, the increased larval size that we observed from early larval development might indirectly result from *aurA* loss-of-function in the ring gland. We could not validate this hypothesis as inactivation of *aurA* by RNAi using ubiquitous, ring gland- or fat body-specific GAL4 did not produce enlarged larvae (data not shown). Nevertheless, quantification of the two major ecdysteroids, 20E and Maki-A, showed that although *aurA^{lof}* mutants can produce basal levels of ecdysteroids, they are unable to produce the major peak required in wandering L3 larvae to pupariate. This result reaffirms our idea that AurA function in the ring gland is necessary for ecdysteroids production peaks and indirectly for early systemic larval growth control. As a consequence, enlarged *aurA* mutant larvae reaches the *drosophila* “critical weight” faster, where feeding is no longer necessary (for review see (Edgar, 2006)), and should pupariate earlier than controls. On the contrary, we observed that *aurA^{lof}* mutant larvae are characterized by a prolonged L3 stage and consequently a delay in pupariation. This phenotype is directly correlated with the absence of an ecdysteroids peak in wandering L3 mutant larvae. Furthermore, we validated that the pupariation delay can be induced by inactivation of *aurA* in the ring gland and not in peripheral tissues as central brain, fat body or wing disc (Sup. Fig. 4). Although we could not detect this major ecdysteroids peak, *aurA* mutant larvae are still able to pupariate. This observation may highlight the limit of ecdysteroids quantification which require a large quantity of larvae to be efficient, however, as *aurA^{lof}* mutant larvae show a prolonged L3 stage, they are heterogeneous in term of larval

timing and the major peak of ecdysteroids might not be present in enough larvae to be detected. Or it may also highlight the fact that this major ecdysteroids peak is not the unique pupariation commitment peak. Indeed, smaller ecdysteroids peaks precede the major one (Warren et al., 2009; Lavrynenko et al., 2015) and could also act as commitment peak (Warren et al., 2009).

The pupariation delay results in a prolonged L3 stage during which most larval tissue development is undertaken. AurA kinase function is essential in cell cycle regulation and not surprisingly in larval tissue development also. In absence of AurA function, cell cycle speed is cell-autonomously affected in wing disc and inhibits its developmental speed. Indeed, although wing discs are smaller at 120h AEL, they reach a wild type size and morphology in wandering L3 mutant larvae. These results comfort our hypothesis that, in absence of AurA kinase activity, wing discs benefit from the prolonged L3 stage to compensate for being developmentally delayed.

The prolonged L3 stage observed in all *aurA^{lof}* mutants is also associated with appearance of enlarged brain lobes in delayed L3 larvae. Nonetheless, these brain lobes are actually smaller in early larval stages, which can be explained by defects in NB-cell lineage. Indeed, loss of *aurA* affects NB asymmetric cell division and give rise to over-proliferative NB-GMC-like cells (Lee et al., 2006; Wang et al., 2006) which do not provide the normal GMC and/or neurons number to fill the central brain. These cells are probably unable to respond to the microenvironment of the central brain that normally controls the number of NB divisions during larval development (Homem and Knoblich, 2012; Lim et al., 2017) and begin to proliferate rapidly and indefinitely. Indeed, the number of dividing NB-GMC-like cells is remarkably high taking in account that cell cycle length is decreased in Dpn+ cells of *aurA^{lof}* mutants (Caous et al., 2015; Lee et al., 2006). This over-proliferation phenotype eventually gives rise to enlarged brain lobes correlated with the prolonged L3 stage. Furthermore, when transplanted in the abdomen of wild-type *Drosophila* hosts, NB-GMC-like cells embedded in a piece of brain become highly tumorigenic (Caous et al., 2015; Caussin and Gonzalez, 2005; Rossi and Gonzalez, 2015). Surprisingly, we could only reproduce partially this NB phenotype by RNAi using a strong NB GAL4 driver (69B) but not with weaker NB-specific GAL4 drivers *worniu-* or *inscutable-*GAL4 (data not shown). This suggests that AurA cell-autonomous function in NB is not sufficient to explain all its functions in NB asymmetric cell-division and that its functions in other central brain cells such as glial cells (Lim et al., 2017) or in other tissues might also be involved.

Interestingly, although AurA was initially defined as a tumor-suppressor in *Drosophila* larvae, it did not appear to be the case in all developing tissues as no over-proliferation were observed in imaginal discs as described for other tumor-suppressor like Brat, disc large or lethal giant larvae (Gateff, 1994). On the contrary, our results show that in absence of AurA, symmetric cell division is decelerated which decreases larval tissues developmental rate. In mice, it was reported that loss of *aurkA* increases tumor-incidence after 50 to 60 weeks suggesting a possible tumor-suppressor effect (Lu et al., 2008). Because of its shorter developmental timing, this cannot be observed in *Drosophila aurA^{lof}* mutants, which are also pupal-lethal (data not shown and (Lee et al., 2006; Moon and Matsuzaki, 2013; Wang et al., 2006)). These results can be taken as an indication that AurA could be a tumor-suppressor only in the case of asymmetric cell division. Indeed, AurA has a dual role in NB-asymmetric cell division: being a major regulator of cell division but also a regulator of the asymmetry. Loss of AurA induces defective asymmetric segregation of Numb (a determinant of GMC cell fate) and aPKC (a central regulator of cell polarity) as well as a defect of central spindle orientation in NB division (Lee et al., 2006; Wang et al., 2006). Conceptually speaking, it would be interesting to study AurA function in other asymmetric cell divisions, such as adult stem cells, to further validate or invalidate the tumor-suppressor function of *aurA* in *Drosophila*.

Acknowledgements

We are indebted to Aurore Dussert for the help with production of *aurA* CRISPR alleles. We thank Fumio Matsuzaki, Pierre Léopold, Jean-René Hyunh, the Bloomington Stock Center and the DSHB for fly stocks and antibodies. We thank the MRiC (Microscopy Rennes imaging Center). We are grateful to Julien Colombani and Pascal Théron for helpful discussion on phenotypic analyses, Yann Le Cunff for statistical work, Rebecca Smith for English proof-reading and Céline Burcklé for comments on the manuscript. This work was supported by the CNRS, the University of Rennes 1, the Ligue Nationale Contre la Cancer (équipe labélisée 2014-2017). L.V. was supported by the Ligue Nationale Contre la Cancer and the Région Bretagne.

References

Ballard, S.L., Jarolimova, J., Wharton, K.A., 2010. Gbb/BMP signaling is required to maintain energy homeostasis in *Drosophila*. *Developmental Biology* 15:375-385.

- Bertolin, G., Sizaire, F., Herbomel, G., Reboutier, D., Prigent, C., Tramier, M., 2016. A FRET biosensor reveals spatiotemporal activation and functions of aurora kinase A in living cells. *Nature communications* 7, 12674.
- Britton, J.S., Edgar, B.A., 1998. Environmental control of the cell cycle in *Drosophila*: nutrition activates mitotic and endoreplicative cells by distinct mechanisms. *Development* 125, 2149-2158.
- Brown, J.R., Koretke, K.K., Birkeland, M.L., Sanseau, P., Patrick, D.R., 2004. Evolutionary relationships of Aurora kinases: implications for model organism studies and the development of anti-cancer drugs. *BMC evolutionary biology* 4, 39.
- Caldwell, P.E., Walkiewicz, M., Stern, M., 2005. Ras activity in the *Drosophila* prothoracic gland regulates body size and developmental rate via ecdysone release. *Current biology* 15, 1785-1795.
- Caous, R., Pascal, A., Rome, P., Richard-Parpaillon, L., Karess, R., Giet, R., 2015. Spindle assembly checkpoint inactivation fails to suppress neuroblast tumour formation in *aurA* mutant *Drosophila*. *Nature communications* 6, 8879.
- Carmena, M., Earnshaw, W.C., Glover, D.M., 2015. The Dawn of Aurora Kinase Research: From Fly Genetics to the Clinic. *Frontiers in cell and developmental biology* 3, 73.
- Caussinus, E., Gonzalez, C., 2005. Induction of tumor growth by altered stem-cell asymmetric division in *Drosophila melanogaster*. *Nature genetics* 37, 1125-1129.
- Chan, C.S., Botstein, D., 1993. Isolation and characterization of chromosome-gain and increase-in-ploidy mutants in yeast. *Genetics* 135, 677-691.
- Colombani, J., Andersen, D.S., Boulan, L., Boone, E., Romero, N., Virolle, V., Texada, M., Leopold, P., 2015. *Drosophila* Lgr3 Couples Organ Growth with Maturation and Ensures Developmental Stability. *Current biology* 25, 2723-2729.
- Colombani, J., Andersen, D.S., Leopold, P., 2012. Secreted peptide Dilp8 coordinates *Drosophila* tissue growth with developmental timing. *Science* 336, 582-585.
- Colombani, J., Bianchini, L., Layalle, S., Pondeville, E., Dauphin-Villemant, C., Antoniewski, C., Carre, C., Noselli, S., Leopold, P., 2005. Antagonistic actions of ecdysone and insulins determine final size in *Drosophila*. *Science* 310, 667-670.
- Cowley, D.O., Rivera-Perez, J.A., Schliekelman, M., He, Y.J., Oliver, T.G., Lu, L., O'Quinn, R., Salmon, E.D., Magnuson, T., Van Dyke, T., 2009. Aurora-A kinase is essential for bipolar spindle formation and early development. *Molecular and cellular biology* 29, 1059-1071.
- Damodaran, A.P., Vaufrey, L., Gavard, O., Prigent, C., 2017. Aurora A Kinase Is a Priority Pharmaceutical Target for the Treatment of Cancers. *Trends in pharmacological sciences*.
- Danielsen, E.T., Moeller, M.E., Yamanaka, N., Ou, Q., Laursen, J.M., Soenderholm, C., Zhuo, R., Phelps, B., Tang, K., Zeng, J., Kondo, S., Nielsen, C.H., Harvald, E.B., Faergeman, N.J., Haley, M.J., O'Connor, K.A., King-Jones, K., O'Connor, M.B., Rewitz, K.F., 2016. A *Drosophila* Genome-Wide Screen Identifies Regulators of Steroid Hormone Production and Developmental Timing. *Developmental cell* 37, 558-570.
- Datta, S., 1995. Control of proliferation activation in quiescent neuroblasts of the *Drosophila* central nervous system. *Development* 121, 1173-1182.
- Delanoue, R., Slaidina, M., Leopold, P., 2010. The steroid hormone ecdysone controls systemic growth by repressing dMyc function in *Drosophila* fat cells. *Developmental cell* 18, 1012-1021.
- Delanoue, R., Meschi, E., Agrawal, N., Mauri, A., Tsatskis, Y., McNeill, H., Léopold, P., 2016. *Drosophila* insulin release is triggered by adipose Stunted ligand to brain Methuselah receptor. *Science* 353(6307):1553-1556.
- Ding, R., Weynans, K., Bossing, T., Barros, C.S., Berger, C., 2016. The Hippo signalling pathway maintains quiescence in *Drosophila* neural stem cells. *Nature communications* 7, 10510.

- Dutertre, S., Cazales, M., Quaranta, M., Froment, C., Trabut, V., Dozier, C., Mirey, G., Bouche, J.P., Theis-Febvre, N., Schmitt, E., Monsarrat, B., Prigent, C., Ducommun, B., 2004. Phosphorylation of CDC25B by Aurora-A at the centrosome contributes to the G2-M transition. *Journal of cell science* 117, 2523-2531.
- Ebens, A.J., Garren, H., Cheyette, B.N., Zipursky, S.L., 1993. The *Drosophila* anachronism locus: a glycoprotein secreted by glia inhibits neuroblast proliferation. *Cell* 74, 15-27.
- Edgar, B.A., 2006. How flies get their size: genetics meets physiology. *Nature reviews. Genetics* 7, 907-916.
- Furuta, T., Baillie, D.L., Schumacher, J.M., 2002. *Caenorhabditis elegans* Aurora A kinase AIR-1 is required for postembryonic cell divisions and germline development. *Genesis* 34, 244-250.
- Garelli, A., Heredia, F., Casimiro, A.P., Macedo, A., Nunes, C., Garcez, M., Dias, A.R., Volonte, Y.A., Uhlmann, T., Caparros, E., Koyama, T., Gontijo, A.M., 2015. Dilp8 requires the neuronal relaxin receptor Lgr3 to couple growth to developmental timing. *Nature communications* 6, 8732.
- Gateff, E., 1994. Tumor suppressor and overgrowth suppressor genes of *Drosophila melanogaster*: developmental aspects. *The International journal of developmental biology* 38, 565-590.
- Gatti, M., Baker, B.S., 1989. Genes controlling essential cell-cycle functions in *Drosophila melanogaster*. *Genes & development* 3, 438-453.
- Glover, D.M., Leibowitz, M.H., McLean, D.A., Parry, H., 1995. Mutations in aurora prevent centrosome separation leading to the formation of monopolar spindles. *Cell* 81, 95-105.
- Green, P., Hartenstein, A.Y., Hartenstein, V., 1993. The embryonic development of the *Drosophila* visual system. *Cell and tissue research* 273, 583-598.
- Hartenstein, V., Campos-Ortega, J.A., 1984. Early neurogenesis in wild-type *Drosophila melanogaster*. *Wilhelm Roux's archives of developmental biology* 193, 308-325.
- Herboso, L., Oliveira, M.M., Talamillo, A., Pérez, C., González, M., Martín, D., Sutherland, J.D., Shingleton, A.W., Mirth, C.K., Barrio, R., 2015. Ecdysone promotes growth of imaginal discs through the regulation of Thor in *D. melanogaster*. *Scientific reports* 22:12383.
- Homem, C.C., Knoblich, J.A., 2012. *Drosophila* neuroblasts: a model for stem cell biology. *Development* 139, 4297-4310.
- Hsu, J.Y., Sun, Z.W., Li, X., Reuben, M., Tatchell, K., Bishop, D.K., Grushcow, J.M., Brame, C.J., Caldwell, J.A., Hunt, D.F., Lin, R., Smith, M.M., Allis, C.D., 2000. Mitotic phosphorylation of histone H3 is governed by Ipl1/aurora kinase and Glc7/PP1 phosphatase in budding yeast and nematodes. *Cell* 102, 279-291.
- Ito, K., Hotta, Y., 1992. Proliferation pattern of postembryonic neuroblasts in the brain of *Drosophila melanogaster*. *Developmental biology* 149, 134-148.
- Jeon, H.Y., Lee, H., 2013. Depletion of Aurora-A in zebrafish causes growth retardation due to mitotic delay and p53-dependent cell death. *The FEBS journal* 280, 1518-1530.
- Kang, K.H., Reichert, H., 2015. Control of neural stem cell self-renewal and differentiation in *Drosophila*. *Cell and tissue research* 359, 33-45.
- Koyama, T., Mirth, C.K., 2016. Growth-blocking peptides as nutrition-sensitive signals for insulin secretion and body size regulation. *PLoS Biology* 14:e1002551.
- Lafont, R., Dauphin-Villemant, C., Warren, J.T., Rees, H.H. 2017. *Ecdysteroid Chemistry and Biochemistry*. Elsevier Reference Module in Life Sciences.
- Lai, S.L., Doe, C.Q., 2014. Transient nuclear Prospero induces neural progenitor quiescence. *eLife* 3.
- Lavrynenko, O., Rodenfels, J., Carvalho, M., Dye, N.A., Lafont, R., Eaton, S., Shevchenko, A., 2015. The ecdysteroidome of *Drosophila*: influence of diet and development. *Development* 142:3758-3768.

- Lee, C.Y., Andersen, R.O., Cabernard, C., Manning, L., Tran, K.D., Lanskey, M.J., Bashirullah, A., Doe, C.Q., 2006. Drosophila Aurora-A kinase inhibits neuroblast self-renewal by regulating aPKC/Numb cortical polarity and spindle orientation. *Genes & development* 20, 3464-3474.
- Lim, N.R., Shohayeb, B., Zaytseva, O., Mitchell, N., Millard, S.S., Ng, D.C.H., Quinn, L.M., 2017. Glial-Specific Functions of Microcephaly Protein WDR62 and Interaction with the Mitotic Kinase AURKA Are Essential for Drosophila Brain Growth. *Stem cell reports* 9, 32-41.
- Lioutas, A., Vernos, I., 2013. Aurora A kinase and its substrate TACC3 are required for central spindle assembly. *EMBO reports* 14, 829-836.
- Lu, L.Y., Wood, J.L., Ye, L., Minter-Dykhouse, K., Saunders, T.L., Yu, X., Chen, J., 2008. Aurora A is essential for early embryonic development and tumor suppression. *The Journal of biological chemistry* 283, 31785-31790.
- Macurek, L., Lindqvist, A., Lim, D., Lampson, M.A., Klompaker, R., Freire, R., Clouin, C., Taylor, S.S., Yaffe, M.B., Medema, R.H., 2008. Polo-like kinase-1 is activated by aurora A to promote checkpoint recovery. *Nature* 455, 119-123.
- McBrayer, Z., Ono, H., Shimell, M., Parvy, J.P., Beckstead, R.B., Warren, J.T., Thummel, C.S., Dauphin-Villemant, C., Gilbert, L.I., O'Connor, M.B., 2007. Prothoracicotropic hormone regulates developmental timing and body size in Drosophila. *Developmental cell* 13, 857-871.
- Mirth, C., Truman, J.W., Riddiford, L.M., 2005. The role of the prothoracic gland in determining critical weight for metamorphosis in Drosophila melanogaster. *Current biology* 15, 1796-1807.
- Moon, W., Matsuzaki, F., 2013. Aurora A kinase negatively regulates Rho-kinase by phosphorylation in vivo. *Biochemical and biophysical research communications* 435, 610-615.
- Ohhara, Y., Kobayashi, S., Yamanaka, N., 2017. Nutrient-dependent endocycling in steroidogenic tissue dictates timing of metamorphosis in Drosophila melanogaster. *PLoS Genetics* 13:e1006583.
- Park, Y., Filippov, V., Gill, S.S., Adams, M.E., 2002. Deletion of the ecdysis-triggering hormone gene leads to lethal ecdysis deficiency. *Development* 129, 493-503.
- Petersen, J., Paris, J., Willer, M., Philippe, M., Hagan, I.M., 2001. The S. pombe aurora-related kinase Ark1 associates with mitotic structures in a stage dependent manner and is required for chromosome segregation. *Journal of cell science* 114, 4371-4384.
- Pinyol, R., Scrofani, J., Vernos, I., 2013. The role of NEDD1 phosphorylation by Aurora A in chromosomal microtubule nucleation and spindle function. *Current biology : CB* 23, 143-149.
- Pugacheva, E.N., Jablonski, S.A., Hartman, T.R., Henske, E.P., Golemis, E.A., 2007. HEF1-dependent Aurora A activation induces disassembly of the primary cilium. *Cell* 129, 1351-1363.
- Reboutier, D., Troadec, M.B., Cremet, J.Y., Chauvin, L., Guen, V., Salaun, P., Prigent, C., 2013. Aurora A is involved in central spindle assembly through phosphorylation of Ser 19 in P150Glued. *The Journal of cell biology* 201, 65-79.
- Riddiford, L.M., 1993. Hormones and Drosophila Development. *The Development of Drosophila melanogaster*. Bate M. Cold Spring Harbor Laboratory Press, 899-939
- Rossi, F., Gonzalez, C., 2015. Studying tumor growth in Drosophila using the tissue allograft method. *Nature protocols* 10, 1525-1534.
- Royzman, I., Whittaker, A.J., Orr-Weaver, T.L., 1997. Mutations in Drosophila DP and E2F distinguish G1-S progression from an associated transcriptional program. *Genes & development* 11, 1999-2011.

- Sardon, T., Peset, I., Petrova, B., Vernos, I., 2008. Dissecting the role of Aurora A during spindle assembly. *The EMBO journal* 27, 2567-2579.
- Sasai, K., Parant, J.M., Brandt, M.E., Carter, J., Adams, H.P., Stass, S.A., Killary, A.M., Katayama, H., Sen, S., 2008. Targeted disruption of Aurora A causes abnormal mitotic spindle assembly, chromosome misalignment and embryonic lethality. *Oncogene* 27, 4122-4127.
- Schumacher, J.M., Ashcroft, N., Donovan, P.J., Golden, A., 1998. A highly conserved centrosomal kinase, AIR-1, is required for accurate cell cycle progression and segregation of developmental factors in *Caenorhabditis elegans* embryos. *Development* 125, 4391-4402.
- Seki, A., Coppinger, J.A., Jang, C.Y., Yates, J.R., Fang, G., 2008. Bora and the kinase Aurora a cooperatively activate the kinase Plk1 and control mitotic entry. *Science* 320, 1655-1658.
- Shearn, A., Garen, A., 1974. Genetic control of imaginal disc development in *Drosophila*. *Proceedings of the National Academy of Sciences of the United States of America* 71, 1393-1397.
- Sousa-Nunes, R., Yee, L.L., Gould, A.P., 2011. Fat cells reactivate quiescent neuroblasts via TOR and glial insulin relays in *Drosophila*. *Nature* 471, 508-512.
- Tsuji, T., Hasegawa, E., Isshiki, T., 2008. Neuroblast entry into quiescence is regulated intrinsically by the combined action of spatial Hox proteins and temporal identity factors. *Development* 135, 3859-3869.
- Voigt, A., Pflanz, R., Schäfer, U., Jäckle, H., 2002. Perlecan participates in proliferation of quiescent *Drosophila* neuroblasts. *Developmental Dynamics* 224:403-412.
- Wang, H., Somers, G.W., Bashirullah, A., Heberlein, U., Yu, F., Chia, W., 2006. Aurora-A acts as a tumor suppressor and regulates self-renewal of *Drosophila* neuroblasts. *Genes & development* 20, 3453-3463.
- Warren, J.T., O'Connor, M.B., Gilbert, L.I., 2009. Studies on the Black Box: incorporation of 3-oxo-7-dehydrocholesterol into ecdysteroids by *Drosophila melanogaster* and *Manduca sexta*. *Insect biochemistry and molecular biology* 39:677-687.
- Warren, J.T., Yerushalmi, Y., Shimell, M.J., O'Connor, M.B., Restifo, L.L., Gilbert, L.I., 2006. Discrete pulses of molting hormone, 20-hydroxyecdysone, during late larval development of *Drosophila melanogaster*: correlations with changes in gene activity. *Developmental dynamics* 235, 315-326.
- Wirtz-Peitz, F., Nishimura, T., Knoblich, J.A., 2008. Linking cell cycle to asymmetric division: Aurora-A phosphorylates the Par complex to regulate Numb localization. *Cell* 135, 161-173.
- Xu, T., Rubin, G.M., 1993. Analysis of genetic mosaics in developing and adult *Drosophila* tissues. *Development* 117, 1223-1237.
- Yao, L.J., Zhong, Z.S., Zhang, L.S., Chen, D.Y., Schatten, H., Sun, Q.Y., 2004. Aurora-A is a critical regulator of microtubule assembly and nuclear activity in mouse oocytes, fertilized eggs, and early embryos. *Biology of reproduction* 70, 1392-1399.
- Yoon, Y., Cowley, D.O., Gallant, J., Jones, S.N., Van Dyke, T., Rivera-Perez, J.A., 2012. Conditional Aurora A deficiency differentially affects early mouse embryo patterning. *Developmental biology* 371, 77-85.

Figure legends

Figure 1: Aurora-A loss of kinase activity affects drosophila larval development speed.

A) Representation of AurA proteins encoded by the wild-type and allelic series of *aurA* mutants. B) Western blots of protein extracts from brains using an anti-AurA antibody (top panel) and an actin antibody (lower panel). AurA is not detected in *aurAST* and *aurA^{3A}* while it is at the expected size in *w¹¹¹⁸*, *aurA^{ST/+}*, *aurA⁸⁸³⁹*, *aurA^{3C}* and *aurA¹⁴⁶⁴¹*. C) Graph of percentage of larvae that have pupariated at the given hours after egg laying (AEL). Pupariation is delayed in all *aurA* mutant genetic backgrounds: *aurA^{3A/ST}* (200 larvae, 2 experiments), *aurA^{8839/ST}* (191 larvae, 2 experiments), *aurA^{3C/ST}* (176 larvae, 2 experiments) and *aurA^{14641/ST}* (108 larvae, 2 experiments) compared to *w¹¹¹⁸* (977 larvae, 3 experiments). D) Scheme of the larval developmental time scale: L1, L2, early L3, late L3 and wandering L3 are indicated. Morphology of anterior and posterior spiracles to stage the larvae, independently from AEL time points, is represented for L1, L2, early L3 and late L3 stages. E) Percentage of different larval stages and pupae observed in *w¹¹¹⁸*, *aurA^{3A/ST}* and *aurA^{8839/ST}* mutants at given AEL time points during larval development. At each time points, two experiments were at least performed and between 24 and 244 larvae were staged for L1 (purple), L2 (green), early L3 (yellow), late L3 (orange), wandering L3 (red) and pupae (blue).

Figure 1

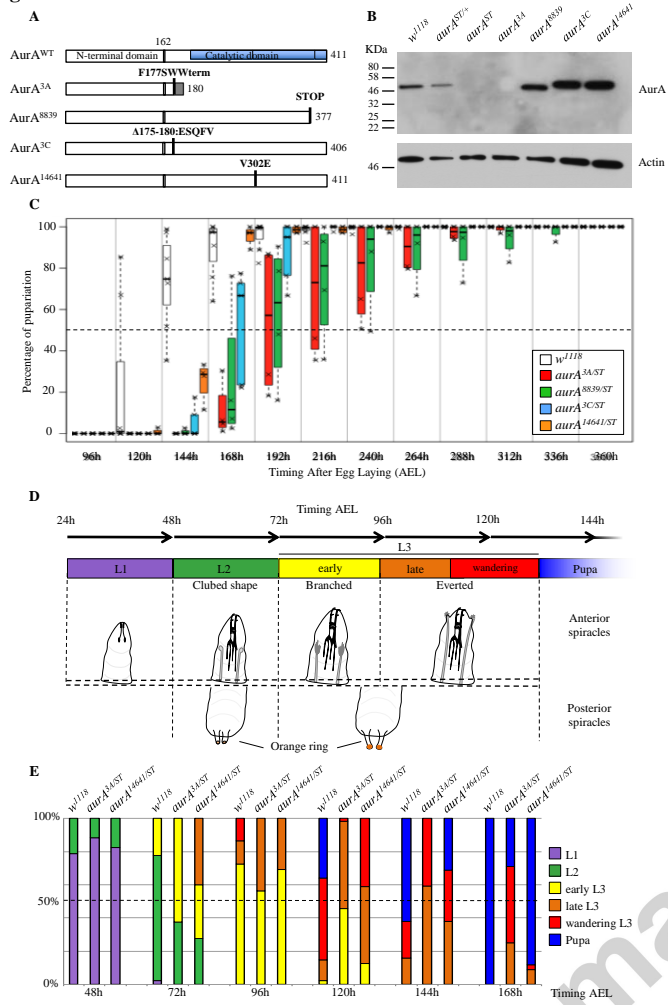


Figure 2

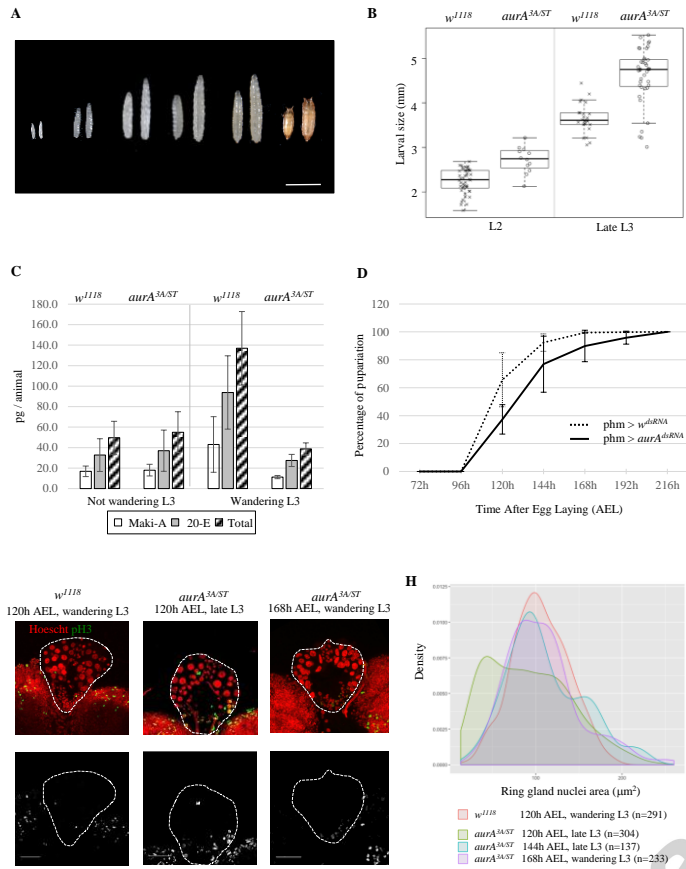


Figure 3

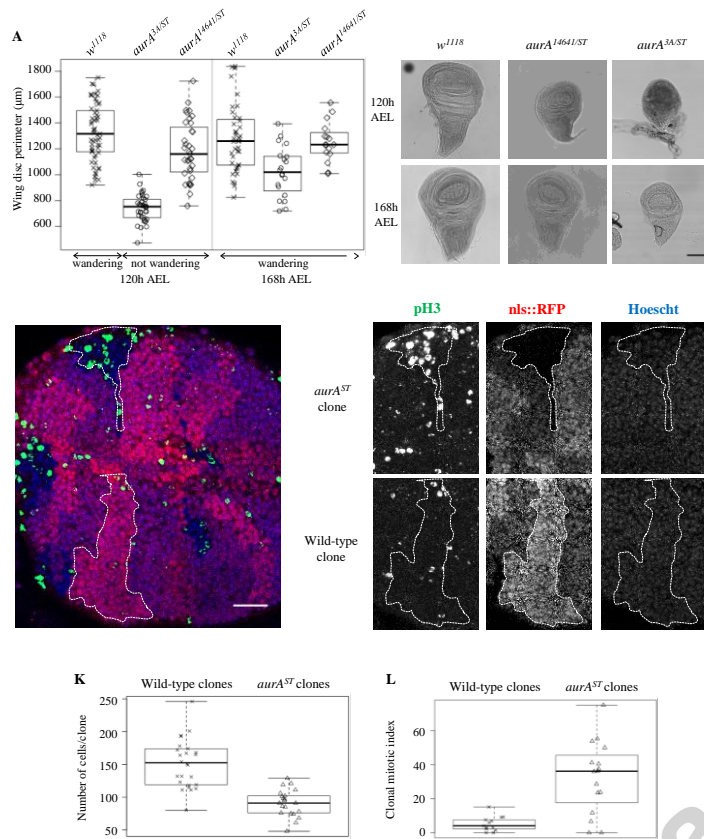
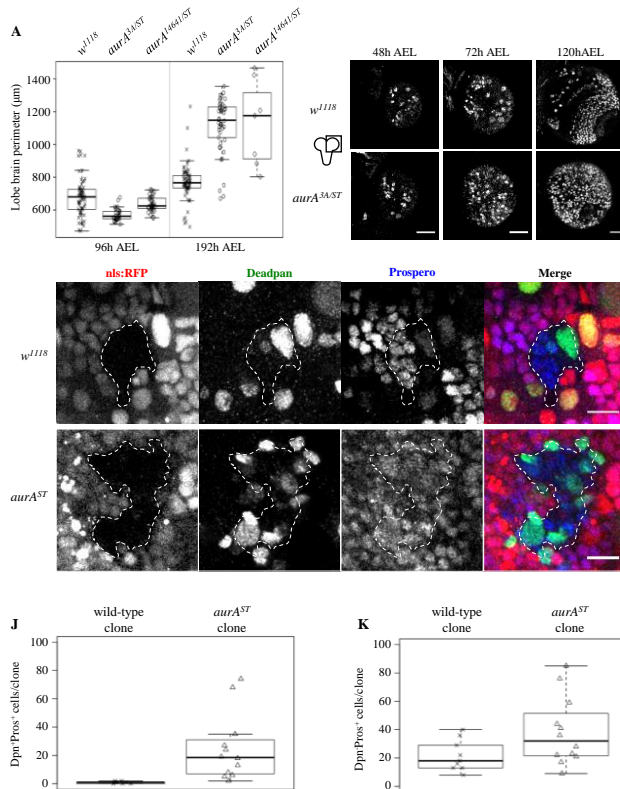


Figure 4



Sup. figure 1: *aurA* alleles are kinase dead mutants.

A) AurA mRNA is detected in all mutants, but in the deletion *aurAST*, at the expected size (conventional RT-PCR). B) AurA polyclonal antibody recognizes wild-type AurA protein and bacteria expressed and purified AurA^{3A} isoform. No protein is detected in *aurA^{3A}* mutant brains. C) *In vitro* AurA kinase assay and corresponding western blot illustrating the abundance of a Ser10-positive band on histone H3 with wild-type AurA and the lack of detectable kinase activity with all mutant isoforms produced *in vitro*.

Figure 2: AurA kinase activity is required in the ring gland to control ecdysteroids production and developmental rate.

A) DIC pictures of *w¹¹¹⁸* (x) and *aurA^{3A/ST}* (o) larvae at 48h, 72h, 96h, 120h and 144h AEL and pupae. Loss of AurA function results in increased larval size easily visible from 72h AEL. B) Box plots showing that larval size of *aurA^{3A/ST}* larvae is bigger than of *w¹¹¹⁸* at 72h AEL ($p=1.01 \times 10^{-8}$, *w¹¹¹⁸* n=105, *aurA^{3A/ST}* n=48, at least 2 experiments) and 120h AEL

($p=1.18 \times 10^{-15}$, w^{1118} $n=106$, $aurA^{3A/ST}$ $n=43$, at least 2 experiments). C) Ecdysteroids content of not wandering *versus* wandering L3 larvae in control (w^{1118}) and $aurA^{lof}$ mutants ($aurA^{3A/ST}$). Quantification by LC-MS/MS of Makisterone-A (Maki-A, white square) and 20-Hydroxyecdysone (20-E, grey square) MS-L/MS are presented as pg/animal. Values are mean \pm s.d. (not wandering w^{1118} : 9 exp, 467 larvae; wandering w^{1118} : 7 exp, 353 larvae; not wandering $aurA^{3A/ST}$: 15 exp, 561 larvae; wandering $aurA^{3A/ST}$: 3 exp, 142 larvae). D) Graph of percentage of larvae that have pupariated at the given hours after egg laying when RNAi against $aurA$ (dashed line, 386 larvae) or *white* (continuous line, 831 larvae) is induced in prothoracic gland using *phm*-GAL4 driver (5 experiments, values are mean \pm s.d.) E-G') 30 μ m confocal projection of w^{1118} 120h AEL (E and E'), $aurA^{3A/ST}$ 120h AEL (F and F') and $aurA^{3A/ST}$ 168h AEL (G and G') ring glands showing mitotic (pH3 positive, green in E'-F') nuclei (Hoescht, red in E-F). Note the higher amount of positive pH3 nuclei in both ring gland and central brains of $aurA^{3A/ST}$ mutants at 120h AEL. H) Histogram showing the density of prothoracic gland nuclei in function of their measured area in w^{1118} 120h AEL and $aurA^{3A/ST}$ 120h, 144h and 168h AEL. Note that the density of $aurA^{3A/ST}$ tends to resemble the Gaussian distribution of control ones ($n_{nuclei}=291$, 8 ring glands) in 144h AEL ($p=0.06$, $n_{nuclei}=137$, 4 ring glands) and 168h AEL larvae ($p=0.30$, $n_{nuclei}=233$, 7 ring glands) but not in 120h AEL ($p=1.40 \times 10^{-10}$, $n_{nuclei}=304$, 7 ring glands). Scale bars are 3mm in A and 50 μ m in E-G'.

Sup. figure 2: $aurA$ mutant larvae are bigger from 72h AEL (A) and from L2 stage (B).

A) Box plots of larval size at different developmental times points AEL for w^{1118} (x), $aurA^{3A/ST}$ (o) and $aurA^{14641/ST}$ (\diamond) genotypes (n are comprised between 24 and 105, at least two experiments per time points). $aurA^{lof}$ mutants are smaller at 48h AEL ($aurA^{3A/ST}$ $p=1.4 \times 10^{-4}$; $aurA^{14641/ST}$, $p=8.6 \times 10^{-10}$) but quickly become bigger from 72h AEL ($aurA^{3A/ST}$, $p=1.01 \cdot 10^{-8}$; $aurA^{14641/ST}$, $p=3.28 \times 10^{-13}$) than controls. B) Box plots of larval size at larval stages for w^{1118} (x), $aurA^{3A/ST}$ (o) and $aurA^{14641/ST}$ (\diamond) genotypes (n are comprised between 6 and 85, at least two experiments per stage points). $aurA^{lof}$ mutants are bigger from the L2 stage ($aurA^{3A/ST}$, $p=3.7 \times 10^{-4}$; $aurA^{14641/ST}$, $p=2.4 \times 10^{-4}$) and stay bigger until the pupal stage ($aurA^{3A/ST}$, $p=3.68 \times 10^{-7}$; $aurA^{14641/ST}$, $p=2.26 \times 10^{-10}$). Note that during L3 stage, the difference is mostly abolished which suggests that the early L3 stage is prolonged ($aurA^{3A/ST}$, $p=0.01$; $aurA^{14641/ST}$, $p=0.013$). During this stage, larvae are still growing which explain the high variability among larvae size.

Sup. figure 3: AurA is required for ecdysteroids release and ring gland development.

A-B) Time course of ecdysteroids content of larvae in control (w^{1118} , A) and $aurA^{lof}$ mutants ($aurA^{3A/ST}$, B) during larval development from 72h AEL to up 192h AEL. Quantification by LC-MS/MS of Makisterone-A (Maki-A, white square) and 20-Hydroxyecdysone (20-E, grey square) MS-L/MS are presented as pg/animal. Values are mean \pm s.d. (72h AEL w^{1118} : 3 exp, 161 larvae; 96h AEL w^{1118} : 5 exp, 231 larvae; 108h AEL w^{1118} : 4 exp, 226 larvae; 120h AEL w^{1118} : 4 exp, 182 larvae; 144h AEL w^{1118} : 4 exp, 181 larvae; 72h AEL $aurA^{3A/ST}$: 2 exp, 116 larvae; 96h AEL $aurA^{3A/ST}$: 4 exp, 150 larvae; 108h AEL $aurA^{3A/ST}$: 2 exp, 105 larvae; 120h AEL $aurA^{3A/ST}$: 3 exp, 122 larvae; 132h AEL $aurA^{3A/ST}$: 2 exp, 57 larvae; 144h AEL $aurA^{3A/ST}$: 4 exp, 127 larvae; 168-192h AEL $aurA^{3A/ST}$: 3 exp, 142 larvae). C) Box plots showing that ring gland perimeters are bigger in w^{1118} (n=36) compared to $aurA^{3A/ST}$ at 120h AEL (p=1.14x10⁻⁵, n=31, three experiments). D) Box plots showing that the mitotic index (% of pH3 positive nuclei/total nuclei) is higher in $aurA^{3A/ST}$ (n=21) ring gland compared to w^{1118} (n=26, 2 experiments, p=2.28x10⁻⁷).

Sup. figure 4: Pupariation delay is not observed when *aurA* is inactivated in other tissues than the ring gland.

A-F) Graphs of percentage of larvae that have pupariated at the given hours after egg laying when RNAi against *aurA* (dashed line) or *white* (continuous line) is induced ubiquitously using 69B-GAL4 (A, 5 experiments, n_{larvae}= 1181 for *white*^{dsRNA}, n_{larvae}= 634 for *aurA*^{dsRNA}), in peripheral tissues using *ppl*-GAL4 (B, 3 experiments, n_{larvae}= 660 for *white*^{dsRNA}, n_{larvae}= 232 for *aurA*^{dsRNA}), in the fat body using *lpp*-GAL4 (C, 2 experiments, n_{larvae}= 236 for *white*^{dsRNA}, n_{larvae}= 121 for *aurA*^{dsRNA}), in larval neuroblasts using *wor*-GAL4 (D, 4 experiments, n_{larvae}= 343 for *white*^{dsRNA}, n_{larvae}= 271 for *aurA*^{dsRNA}) or in wing discs using *pdm2*-GA4 (E, 3 experiments, n_{larvae}= 778 for *white*^{dsRNA}, n_{larvae}= 270 for *aurA*^{dsRNA}) or *ser*-GAL4 (F, 3 experiments, n_{larvae}= 702 for *white*^{dsRNA}, n_{larvae}= 318 for *aurA*^{dsRNA}). All crosses gave viable and fertile adults without obvious phenotypes excepted wing margin shafts duplication for *ser*>*aurA*^{dsRNA}. Values are mean \pm s.d.

Figure 3: Aurora-A loss of function inhibits developmental wing disc growth rate.

A) Box plots representing wing disc perimeters at 120h and 168h AEL for w^{1118} and $aurA^{3A/ST}$ not wandering and wandering larvae as indicated. At 120h AEL, wing disc are smaller in late L3 $aurA^{3A/ST}$ (n=37, p=4.72x10⁻⁶) and $aurA^{14641/ST}$ (n=35, p=5.26x10⁻³) mutant larvae compared to wild-type wandering L3 larvae (n=57). At 168h AEL, $aurA^{3A/ST}$ (n=20, p=2x10⁻³) and $aurA^{14641/ST}$ (n=16, p=0.94) mutant wing discs have caught up with control ones

(n=40). At least two experiments were performed. B-G) DIC pictures of w^{1118} (B,E), $aurA^{14641/ST}$ (C,F) and $aurA^{3A/ST}$ (D,G) wing disc at 120h and 168h AEL. H-J'') 5 μ m confocal projection of wing disc with focus on a wild-type clone (double positive for nls::RFP, J') and an $aurA^{ST}$ clone (negative for nls::RFP, I'). Note that $aurA^{ST}$ clones have less cells (marked with Hoescht, blue in I'') and more nuclei positive for pH3 a marker of pro-metaphase (green in I) compared to wild-type clone (J-J''). K) Box plots showing the numbers of Hoescht positive cells per clones. $aurA^{ST}$ clones (n=16) have less cells than wild-type twin-spot clones (n=12) in wing disc ($p=3.13 \times 10^{-7}$). L) Box plots showing that the clonal mitotic index (% of pH3 positive nuclei/total nuclei per clone) is higher in $aurA^{ST}$ wing disc clones (n=16) compared to wild-type ones (n=12, $p=0.00125$). Scale bars are 100 μ m in B-G and 10 μ m in H-J'').

Supplementary figure 5: Enlarged brain size does not result from bigger larval size.

A) Box plots of larval size at 120h AEL for w^{1118} (x, n=45), $aurA^{3A/ST}$ (\diamond , n=24) and *avalanche* (avl)^{dsRNA} (*, n=13) genotypes. Size are similar between $aurA^{3A/ST}$ and avl ^{dsRNA} ($p=0.9126$) and bigger to controls ($aurA^{3A/ST}$, $p=7.23 \times 10^{-16}$; avl ^{dsRNA}, $p=7.6 \times 10^{-12}$). B) Box plots showing lobe brain perimeters at different developmental time points. At 120h AEL, brains are smaller in $aurA^{3A/ST}$ (n=80) and avl ^{dsRNA} (n=10) compared to w^{1118} (n=113, $p<2.2 \times 10^{-16}$ and $p=1.84 \times 10^{-7}$, respectively). At 144h AEL and 168h AEL, brains of $aurA^{3A/ST}$ (n=116 and 80) are now bigger compared to w^{1118} (n=65 and 58, $p=1.8 \times 10^{-4}$ and 3.25×10^{-6} , respectively). On the contrary, brains of avl ^{dsRNA} stay smaller (n=10, $p=1.9 \times 10^{-7}$ at 144h AEL and n=11, $p=2.4 \times 10^{-4}$ at 168h AEL) certainly due to the fact that *avl* function is essential to development.

Figure 4: AurA loss of function induces proliferation of cells stuck in between NB and GMC-cell identity.

A) Box plots representing lobe brain perimeters at 96h AEL and 192h AEL for w^{1118} and $aurA^{3A/ST}$. Lobe brain perimeters are initially smaller in $aurA^{3A/ST}$ (n=33, $p=2.85 \times 10^{-7}$) and slightly in $aurA^{14641/ST}$ (n=33, $p=0.03$) than in w^{1118} (n=67) at 96h AEL and are eventually bigger later during larval development at 192h AEL ($aurA^{3A/ST}$, n=47, $p=1.68 \times 10^{-13}$, $aurA^{14641/ST}$, n=8 and w^{1118} , n=63, $p=1.79 \times 10^{-4}$). B-G) Confocal projection of 15 μ m of w^{1118} (B-D) and $aurA^{3A/ST}$ (E-G) lobe brains at 48h, 96h and 120h AEL stained for Deadpan (Dpn) a neuroblast cell-identity marker. The number of Dpn⁺ cells increased drastically during larval development to reach a paroxysm at 120h AEL despite the smaller lobe brain size. Note that

the scale bar size is different in B,C,E,F versus to D,G due to the large size of lobe brains at 120h AEL. H-I''') Confocal projection of 5 μ m of wild-type (n=9, H-H''') and *aurA*ST (n=14, I-I''') clones (negative for nls::RFP, H and I) stained for Deadpan (green, H' and I') and Prospero (Pros, blue, H'' and I'') a GMC cell identity marker. Mutant clones are filled with (small nucleus, Dpn⁺ Pros⁺) cells which are not seen in wild-type clones excepted the newly born GMC (white arrow). J) Box plots showing the numbers of (Dpn⁺ Pros⁺) positive cells per clones. (Dpn⁺ Pros⁺) cells are more present in *aurA*ST central brain clones (n=14, p=1.2x10⁻⁴) than in wild-type clones (n=9). K) Box plots showing the numbers of (Dpn⁻ Pros⁺) positive cells per clones. GMC (small nucleus, Dpn⁻ Pros⁺) are detected in the same quantity in *aurA*ST central brain clones (n=14, p=0.069) than in wild-type clones (n=9). Scale bars are 30 μ m in B-G and 10 μ m in H-I.

Sup. figure 6: AurA is required in central brain development

A) Graph of brain lobe perimeters at different developmental larval time points from 48h AEL to 192h AEL. During larval development, *aurA*^{lof} mutant brains are smaller and eventually get bigger than wild-type from 144h AEL for all genotypes: *aurA*^{3A/ST}, *aurA*^{8839/ST}, *aurA*^{3C/ST} and *aurA*^{14641/ST}. For each time points, n_{larvae} is at least of 8 with an average of 47 and at least two experiments were performed. There is no significantly differences at 48h AEL (p>0.0125). At 96h AEL, brains are significantly bigger in *aurA*^{lof} (excepted *aurA*^{14641/ST}, p=0.03) than *w*¹¹¹⁸ ones (p<2.1x10⁻⁴). Finally, at 192h AEL, brains are larger in *aurA*^{lof} than *w*¹¹¹⁸ ones (p<1.7x10⁻⁴). B-G) Confocal projection of 15 μ m of *w*¹¹¹⁸ (B,D,F) and *aurA*^{3A/ST} (C,E,G) lobe brains at 96h, 120h and 168h AEL stained for Dpn (green), a neuroblast cell marker and Pros (red), a GMC marker. Mutant brain lobes are initially smaller and get bigger. They also present defects in their morphology as observed with the lack of clear optic lobe structure. Note that the scale bar size is different in F,G due to the large size of lobe brains at 168h AEL. H-I) Confocal projection of 15 μ m of *w*¹¹¹⁸ (H) and *aurA*^{3A/ST} (I) lobe brains at 120h AEL stained for ELAV a neuronal marker. Note the loss of neurons (ELAV⁺) in *aurA*^{3A/ST}. Scale bars are 30 μ m.

Highlights

- AurA indirectly controls *Drosophila* larval development coordination
- Loss of *aurA* decreases larval tissue development speed
- Loss of *aurA* affects ring gland development speed, which in turns decreases ecdysteroids production
- Enlarged central brain in *aurA* mutants result from both pupariation delay and over-proliferation of pseudo-neuroblasts.

Accepted manuscript